Block Copolymers for Organic Optoelectronics

ARTICLE *in* MACROMOLECULES · NOVEMBER 2009

Impact Factor: 5.8 · DOI: 10.1021/ma901350w

4 AUTHORS, INCLUDING:

Saar Kirmayer
Weizmann Institute of Science
18 PUBLICATIONS **973** CITATIONS
SEE PROFILE

Jeffrey J Urban
Lawrence Berkeley National Laboratory
84 PUBLICATIONS **2,728** CITATIONS
SEE PROFILE

Macromolecules
PERSPECTIVE

Macromolecules **2009**, *42*, 9205–9216 **9205**
DOI: 10.1021/ma901350w

Block Copolymers for Organic Optoelectronics

Rachel A. Segalman,*,†,‡ Bryan McCulloch,† Saar Kirmayer,† and Jeffrey J. Urban‡

†*Department of Chemical Engineering, University of California, Berkeley, California 94720 and*
‡*Materials Science Division, Lawrence Berkeley National Laboratories, Berkeley, California 94720*

Received June 23, 2009; Revised Manuscript Received October 21, 2009

ABSTRACT: While polymers hold significant potential as low cost, mechanically flexible, lightweight large area photovoltaics and light emitting devices (OLEDs), their performance relies crucially on understanding and controlling the morphology on the nanometer scale. The ca. 10 nm length scale of exciton diffusion sets the patterning length scale necessary to affect charge separation and overall efficiency in photovoltaics. Moreover, the imbalance of electron and hole mobilities in most organic materials necessitates the use of multiple components in many device architectures. These requirements for 10 nm length scale patterning in large area, solution processed devices suggest that block copolymer strategies previously employed for more classical, insulating polymer systems may be very useful in organic electronics. This Perspective seeks to describe both the synthesis and self-assembly of block copolymers for organic optoelectronics. Device characterization of these inherently complex active layers remains a significant challenge and is also discussed.

Optimization of organic photovoltaics and light emitting devices relies on controlling the nanoscale morphology of at least two semiconducting materials with different energy level alignments to maximize charge separation, recombination, and transfer.[1,2] The necessity for nanoscale pattern control is most easily exemplified in organic solar cells. These devices are generally made of two materials: an electron donating (p-type) component in which light is absorbed to create an exciton (bound electron−hole pair) and an electron accepting (n-type) component which accepts the electron from the donor. In this scheme, an electron accepting material is a material with lower HOMO and LUMO energy levels than the electron donor. The HOMO (highest occupied molecular orbital) and LUMO (lowest unoccupied molecular orbital) are analogous to the valence and conduction bands often used to describe inorganic semiconductors. When light is absorbed by the material, an electron may be excited from the HOMO (lower energy) to the LUMO (higher energy) with the energy difference between these two energy levels referred to as the band gap. For example, P3HT is commonly used as the predominant light absorber in efficient organic photovoltaics and has a band gap of around 1.85 eV ($\lambda \approx 675$ nm). Tuning the band gap energy is important for the optimization of the device performance because photons with less energy than the band gap will not be captured and any energy that photons carry greater than the band gap will be lost when the excited electron relaxes to the HOMO energy level. On the basis of the solar spectrum, assuming an ideal device, a band gap of around 1.4 eV gives the theoretical maximum efficiency of around 33%.

After photoexcitation and charge separation the electron and hole are then transported back to the appropriate electrodes through the accepting and donating domains, respectively. This process dictates strict geometrical requirements on the device: the donor−acceptor interfaces must be prevalent (occurring every ∼10 nm) so that every created exciton may encounter an interface prior to recombination. Additionally, the donor and acceptor phases must form continuous pathways to the electrodes to allow for efficient charge transport and collection. This 10 nm length scale patterning is difficult to achieve via conventional lithographic patterning techniques or by phase separation of polymer blends. Patterning is also of importance in organic light emitting

*To whom correspondence should be addressed. E-mail: segalman@berkeley.edu.

Professor Rachel A. Segalman is currently an Associate Professor of Chemical Engineering at the University of California, Berkeley, and an Associate Faculty Scientist at Lawrence Berkeley National Laboratories. Segalman earned a B.S. in Chemical Engineering at the University of Texas at Austin and Ph.D. in Chemical Engineering at the University of California, Santa Barbara, under the direction of Professor Edward J. Kramer. After spending a year at the Universite Louis Pasteur, Strasbourg, France, as a Chateaubriand Fellow with Prof. Georges Hadziioannou, she joined the University of California, Berkeley, in 2004. Among other awards, Segalman received a National Science Foundation CAREER award in 2005, a Presidential Early Career Award in Science and Engineering (PECASE) in 2008 and was awarded an Alfred P. Sloan Fellowship in 2009. Her research expertise in polymeric materials includes functional block copolymers, conjugated rod−coil block copolymers, and polymers and nanocomposites for thermoelectric applications. She has also developed expertise in the measurement of structure−property relationships in small and polymeric molecules, focusing particularly on molecular junction measurements.

Published on Web 11/11/2009

Bryan McCulloch received his B.S. in chemical engineering from the University of Washington in 2007. He is currently a doctoral candidate in Chemical Engineering at UC Berkeley working under the direction of Professor Rachel Segalman, focusing on the physics of nanoparticle self-assembly within conjugated rod−coil block copolymers.

Saar Kirmayer received his PhD from the Technion, Haifa Israel in 2008, where he did research at the Materials Engineering Department under the supervision of Professor Gitti Frey. Saar received the Technion postdoctoral fellowship for research on alternative energy sources and is currently a postdoctoral fellow with the Chemical Engineering Department at University of California, Berkeley, and with the Molecular Foundry at the Lawrence Berkeley Laboratory. His work is focusing on studying the effects the morphology as well as the interface properties has on the charge separation process in organic and organic/inorganic hybrid solar cells.

Jeffrey Urban is currently a Staff Scientist at the Molecular Foundry located at Lawrence Berkeley National Laboratories in Berkeley, CA. He received his B.Sc. from Pennsylvania State University in Biochemistry and Molecular Biology. Urban then earned his M.A. and Ph.D. in Physics and Chemistry and Chemical Biology with Prof. Hongkun Park at Harvard University. After obtaining his Ph.D., he then spent two years as a postdoctoral researcher, coadvised by Prof. Christopher B. Murray (University of Pennsylvania) and Prof. Mercouri Kanatzidis (Northwestern University). His research currently focuses on the study of thermal and electrical transport phenomena in the context of energy storage and conversion technologies.

diodes (OLEDs), though the purpose of pattern optimization here generally has to do with balancing transport of electrons and holes toward the center of the device rather than exciton manipulation.

While self-assembly is an alluringly inexpensive route to patterning on the 10 nm length scale of relevance to organic optoelectronics, only recently have successful demonstrations of self-assembly in semiconducting polymers emerged. However, while not optimized for electronic device applications, a clear understanding of the self-assembly behavior of classical coil−coil block copolymers exists,[3] and a great deal of work has been done to control the thin film order of such materials, primarily for nanolithographic applications.[4] Using this knowledge to manipulate the nanoscale patterning of semiconducting block copolymers presents a new challenge due to nonidealities in molecular conformation and mixing interactions commonly present in semiconducting materials. Recently, the expansion of our understanding of block copolymer self-assembly to materials appropriate for organic electronics has been the subject of much interest.

Block copolymers for organic optoelectronics must contain at least two distinct electronic functionalities in the chain. For OLEDs, polymers generally must contain at least electron and hole transporting (and, occasionally, emitting) functionalities while block copolymers for photovoltaics characteristically contain both electron donating and accepting functionalities. These semiconducting properties in polymers can be derived either by conjugation of the polymeric backbone[5] or by attaching semiconducting molecules pendant to the backbone.[6] The compatibility of the syntheses of these types of polymers with block copolymer routes (which must yield well-defined blocks) presents a challenge. Furthermore, conjugation serves to rigidify the backbone to form rodlike chains and introduce liquid crystalline interactions, thereby forming so-called rod−coil block copolymers.[7] A number of stunning and intriguing phases have been observed in similar, but nonconjugated, rod−coil block copolymer systems;[8−12] however, only recently have the phase diagrams and the thermodynamics of rod−coil block copolymer self-assembly been more fully elucidated.[13] Alternatively, small molecule pendant groups are more easily compatible with living polymerization routes but tend to be bulky and crystalline, features which add undesirable kinetic and thermodynamic challenges to self-assembly. Self-assembly alone creates interfaces on the 10 nm length scale and is an exciting platform from which to understand the fundamental role of patterning on device performance, particularly charge separation and recombination events. Optimization of device behavior requires both control over nanodomain orientation and also long-range order to facilitate optimal charge transport. This Perspective will outline recent developments in both controlling semiconducting polymer self-assembly and also the development of block copolymer materials for photovoltaics and OLEDs; the final section will look forward toward the use of block copolymers for understanding

the role of nanostructure in device performance as well as controlling self-assembly for optimal performance.

Conjugated Rod−Coil Block Copolymers

Although self-assembly of conjugated rod−coil block copolymers is a potentially elegant path to achieve the same control over nanoscale structure exercised in classical block copolymer systems, the necessary predictive polymer thermodynamics of semiconducting polymers remains less well studied. In classical block copolymers, the conformational properties of both blocks are characterized by Gaussian chain statistics, and the microphase structure is a compromise between minimizing the interaction energy between unlike blocks and the stretching of the Gaussian coils.[3,14] In conjugated rod−coil block copolymers the rod block has an effectively infinite persistence length and a single orientational vector defining its conformation. The self-assembly of rod−coil systems is further complicated by the anisotropic interactions and liquid crystalline behavior of the rod block. The chain stretching, isotropic Flory−Huggins interaction, and anisotropic rod interactions all impact the equilibrium microphase structure. The interplay between these effects creates equilibrium structures and thermodynamics that are distinct from coil−coil block copolymer systems.

Analytical free energy calculations of rod−coil block copolymer systems predict transitions between nematic, smectic A and C, bilayer, and "puck" phases.[15−19] Alternately, Landau expansions for the free energy in terms of both compositional and orientational order parameters treat rod−coil block copolymers in the weak segregation limit.[20−22] These calculations predict microphase-separated structures as well as nematic and isotropic phases. Self-consistent field theory (SCFT) has also been applied to rod−coil block copolymers.[21−25] These studies have predicted more complex phase diagrams including isotropic, nematic, and lamellar structures for a wide range of compositions across the center of the phase diagram. Arrowhead and bilayer microphases were also predicted for rod-rich systems, while strip or puck morphologies were favored in coil-rich systems.

A major difficulty in experimentally addressing conjugated rod−coil block copolymer self-assembly is the preparation of a suitable model material with which to probe phase transitions. This requires that the system have a low enough Flory−Huggins parameter, and weak enough liquid crystalline interactions, such that phase transitions can be experimentally accessed. In addition, both blocks must have low polydispersity and easy molecular weight control during synthesis. Weakening these thermodynamic interactions may be done by reducing molecular weight to the oligomeric level,[23−25] but frequently the molecular weights required to reduce transitions to less than 300 °C are too short to be useful models for polymeric behavior. Alternatively, weakly segregated rod−coil block copolymers of alkoxy-substituted derivatives of poly(phenylenevinylene) have attracted much interest.[26−32] In this class of materials, the conjugated rod is appropriate for photovoltaic and OLED applications, but the coil block is chosen simply for its ability to provide fundamental information about thermodynamics and self-assembly. Poly(2,5-di(2′-ethylhexyloxy)-1,4-phenylenevinylene)-*b*-polyisoprene (PPV−PI) was the first polymeric weakly segregated system with accessible phase transitions, enabling the construction of the first phase diagram for conjugated rod−coil block copolymer self-assembly, as illustrated in Figures 2 and 3.[26−29] This phase diagram is *qualitatively* different than that of classical coil−coil block copolymers due to the rod interactions. For example, lamellar structures occur at low temperatures and are observed through a broader range of coil fractions than in classical polymers. Hexagonal phases have also been observed in very asymmetric systems.[28,33] As the temperature is increased, the rods and coils begin to mix on a molecular scale, but a nematic phase is stabilized by the predominant rod−rod interactions.[27] At high temperatures, as expected, an isotropic phase is observed. The lack of more complex phases in the weak segregation limit for rod−coil block copolymers probably arises from a combination of the strong rod−rod interactions which disfavor curved interfaces and the very low Flory−Huggins constant. Both features may allow liquid crystalline interactions to dominate phase behavior.[28,29,34] In fact, cylindrical and spherical phases have been observed in related systems with larger Flory−Huggins constants,[30,32,34,35] and even more complex phase space has been observed in analogous oligomeric systems in which the coil block appears to be fully extended.[12,36]

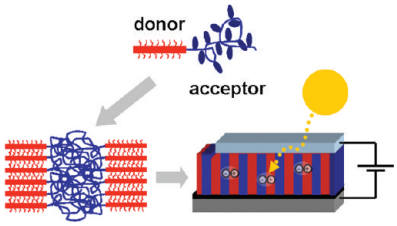

Figure 1. Block copolymer self-assembly may be used to create patterning for charge separation, recombination, and transport on the characteristic 10 nm length scale of exciton diffusion.

The equilibrium phase behavior of coil−coil block copolymers can be parametrized by the volume fraction, ϕ, and the Flory−Huggins interaction between the blocks, χN, where N is the molecular length.[3] In rod−coil block copolymer systems the liquid crystalline interaction and the topological disparity between the rod and the coil polymer require the introduction of two additional parameters. The Maier−Saupe interaction strength, μN, characterizes the aligning interactions between the rod blocks.[7] Additionally, the rod and coil blocks are constrained to occupy the same interfacial area. However, their different scaling dimensions imply that their aspect ratios scale differently with molecular weight, creating a packing frustration due to size mismatch. This is parametrized by a geometrical asymmetry, ν, defined as the ratio between the coil radius of gyration and the rod length.[37,38] For example, hexagonal phases only occur in polymers with sufficiently high asymmetry in both ϕ and ν,[28−30,32] illustrating the critical importance of both terms in determining the microphase structure of rod−coil block copolymers. As a result, phase space in a single rod−coil block copolymer system can only be fully defined in a 4-D phase diagram incorporating both temperature-dependent interaction terms and both of geometrical terms. Furthermore, it has been suggested that in some regimes the Flory−Huggins interactions may dominate phase behavior while in others the rod−rod Maier−Saupe interactions may dominate. As a result, the observed morphology in these systems depends on the ratio of these two parameters,[22,34] with liquid crystalline and nonlamellar structures[33,35] emerging from cases in which the predominant interactions are the Maier−Saupe and Flory−Huggins interactions, respectively.

While nanoscale domain size is important for organic optoelectronics, control over orientation relative to the electrodes may be even more crucial. For example, in the solar cell architecture, nanostructuring may provide a large density of donor−acceptor interfaces to promote charge separation. However, if the p-type (donor) and n-type (acceptor) domains are randomly oriented throughout the remainder of the film, then recombination will be prevalent and device performance will be poor. An optimal photovoltaic device requires not only strong absorption of incident light but also efficient charge separation and good charge transport to the proper electrodes. Therefore, lamellae (stripes)

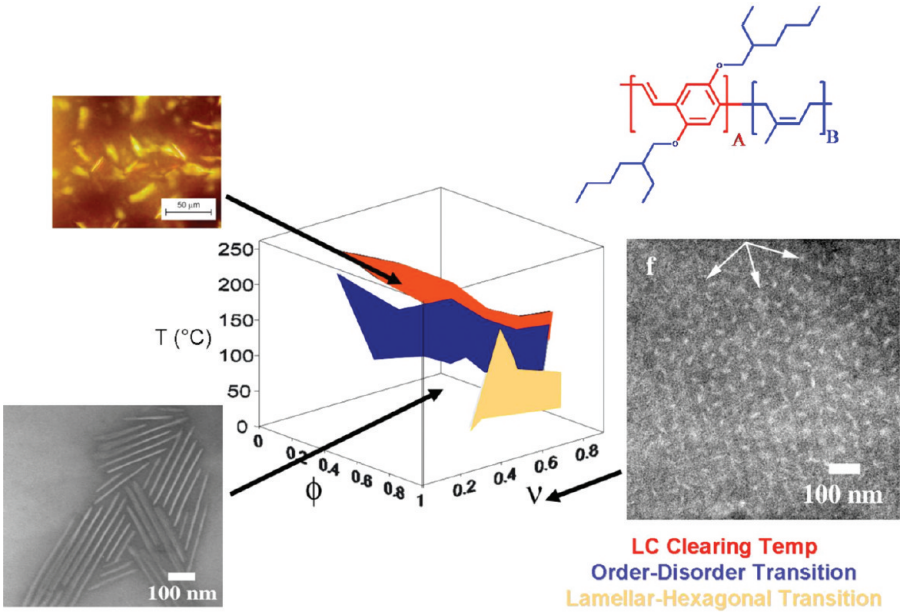

Figure 2. Phase diagram for weakly segregated rod−coil block copolymer. Both the Flory−Huggins block−block interaction parameter and the Maier−Saupe parameter are captured in terms of temperature. The coil volume fraction, ϕ_{coil}, and a geometrical asymmetry term, ν, account for aspect ratio differences between the rod and coil. In this 3D phase diagram, lamellar (illustrated by TEM), hexagonal (TEM), nematic (polarized optical micrograph), and isotropic phases are observed.

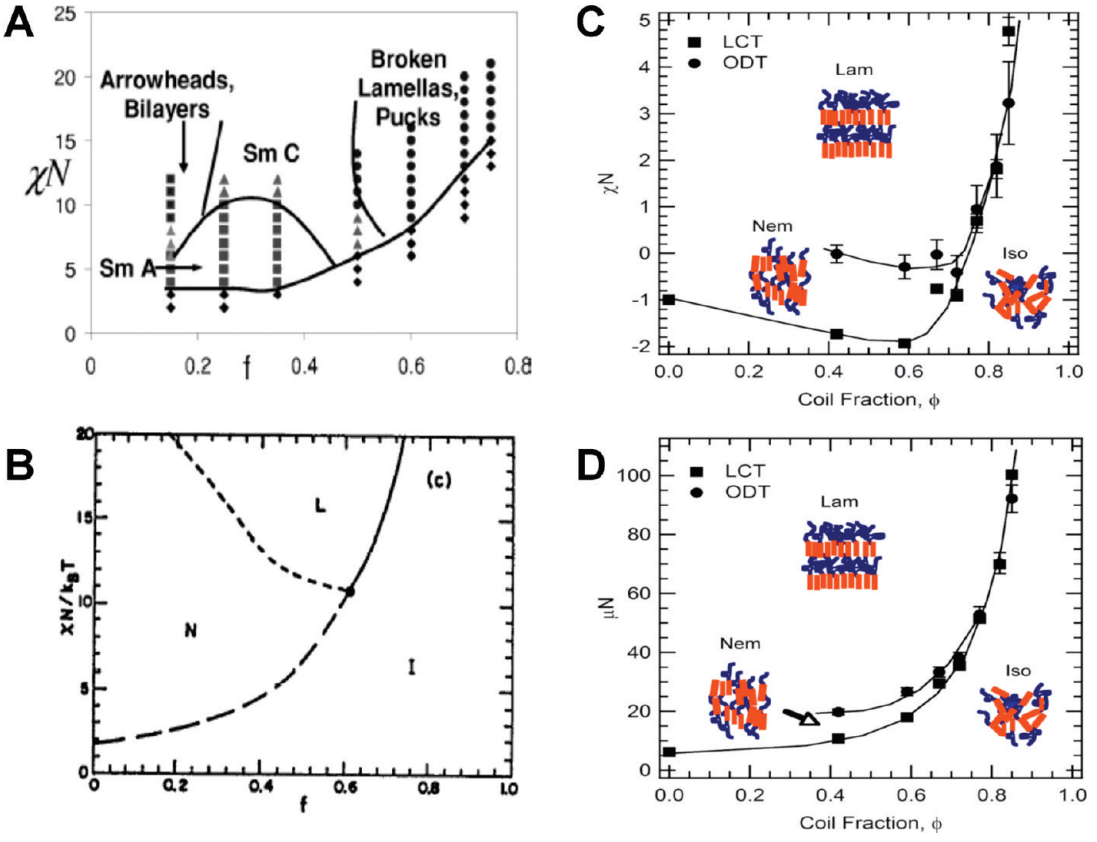

Figure 3. Rod−coil block copolymer phase space depends on two geometrical parameters (volume fraction of coil and geometrical asymmetry) as well as rod−coil interaction (Flory−Huggins interaction strength, χN) and rod−rod alignment interaction strength (Maier−Saupe interaction, μN). Shown here are phase diagrams from mean-field predictions (A: Reprinted with permission from ref 37. Copyright 2004 AIP), Landau predictions (B: Reprinted with permission from ref 20. Copyright 1992 AIP),[20] and a weakly segregated PPV-*b*-PI system in terms of both χN (C) and μN (D).[29]

aligned with their interfaces perpendicular to the electrodes (Figure 1) represents an ideal morphology simultaneously enabling a high density of exciton splitting interfaces along with untrammeled paths for both hole and electron transport out to the proper electrodes. Rod−coil block copolymer lamellae have been demonstrated to align bimodally, both parallel and

perpendicular to the substrate (electrode interfaces), but this orientation depends strongly on thermal history and film thickness.[39−42] In classical block copolymers, control over nanodomain orientation and placement has been an intense focus of research and is the subject of numerous reviews.[4,43−45] For example, block copolymer interfaces perpendicular to an externally applied electric field bear a free energy penalty, and as a result, entire classical block copolymer lamellae and cylinders tend to reorient parallel to the field.[46] In a similar manner, conjugated polymer lamellae can be aligned in a magnetic field.[47] In addition, a variety of surface-based alignment techniques have also been implemented in conjugated homopolymers and may be promising in the block copolymer context. Flow coating can be used during casting to induce order.[39−42] Furthermore, the comprehensive review by Grell and Bradley[48] outlines strategies to achieve alignment in these materials, including direct rubbing of the conjugated layer and casting on top of alignment-inducing substrates. These techniques result in both high degrees of molecular orientation and lead to polarized emission in the case of organic light emitting diodes (OLEDs).

Optical Properties of Conjugated Block Copolymers

Optical spectroscopy is a valuable tool to probe carrier dynamics in solid-state optoelectronic devices. A variety of complementary techniques including steady-state and transient absorption and excitation/emission measurements are powerful tools to study the detailed energy landscape in these systems and electron and hole carrier lifetimes. Moreover, when combined with well-controlled block copolymer morphologies, these spectroscopic tools may be used to study both intra- and interchain charge and energy transfer processes across a variety of time scales (~milliseconds to ~femtoseconds). Judicious selection of the blocks and other system components (i.e., solvent, quencher, etc.) allows for the independent probing of the absorption and emission of individual blocks and an opportunity to observe charge transfer between blocks or entire chains. For example, in the polythiophene-*b*-polyfluorene derivative block copolymer system, poorly solvating solvents lead to aggregation. This morphology favors intrachain energy transfer and quenching of the strong polythiophene emission.[49,50] Similarly, correlations between local structure in diblock polymers and optically induced energy transfer pathways have been established in highly fluorinated copolymer systems, consisting of one block containing an alternating sequence of triphenylamino-disubstituted fluorene with dialkyl-substituted fluorine with a second block consisting of an alternating sequence of benzothiadiazole with dialkylfluorene. In this case, intrachain energy transfer is known to dominate when the polymer is optically excited in solution; however, solid-state measurements performed on thin films of this material implicate both intra- and interchain interactions in both the energetics and carrier lifetime dynamics.[51] These, and many other studies, clearly indicate that self-assembly and local structure are critical design parameters to optimizing the optoelectronic performance of block copolymer systems.[52−59] However, despite this promise, experimental challenges have limited careful correlations between structure and property in ordered diblock copolymer systems, leading to a preponderance of studies on diblock co-oligomers.[23,24,60−63]

Block Copolymers for Organic Photovoltaics (OPVs)

Organic solar cells provide a path to low cost renewable energy generation which offers significant improvements in durability and manufacturing scalability in comparison to traditional silicon cells. Unfortunately, single-component organic solar cells have historically shown low efficiencies. Leveraging the fundamental principles of polymer physics to create highly ordered, multiphase structures whose exciton splitting and charge transport properties are optimized remains both a possibility and a grand challenge.[1,64] Power generation in organic photovotaics may be simplified into three distinct steps: light absorption, charge generation, and charge transport. First, light absorption must be maximized to photogenerate the largest number of electron−hole pairs (excitons) possible. After photoexciation, however, the electron and hole remain strongly electrostatically bound as excitons and must be split to provide free carriers. Because of the low dielectric constant in organic polymers, excitons typically have large binding energies on the order of several tenths of an electronvolt,[65,66] and separate charges are not typically generated. Effective charge separation is known to occur as an exciton encounters a strong electric field. In organic materials, this field can be designed into the material itself, in the form of a donor−acceptor interface. Across this donor−acceptor interface, a large HOMO−LUMO energy level offset (~0.3 eV) is necessary to produce a large enough internal electric field gradient capable of splitting excitons into free electrons and holes. For maximum performance, it is also critical that there be a high density of these donor−acceptor interfaces throughout the active layer, as excitons must diffuse to this interface prior to undergoing radiative and nonradiative decay.

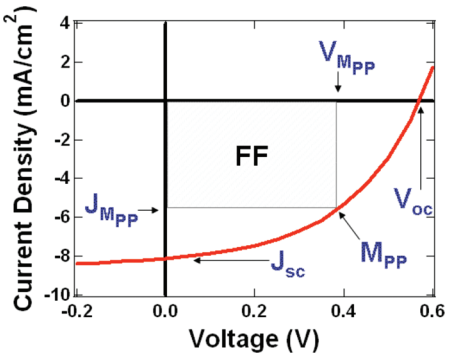

Figure 4. Typical current density vs voltage curves ($J-V$) of an organic solar cell showing the critical values which determine device efficiency. These parameters include the short-circuit current (J_{sc}), open-circuit voltage (V_{oc}), and the current and voltage values for the maximum power point (mpp, J_{mpp} and V_{mpp}). The fill factor (FF) is the ratio of the outlined area defined by the maximum power points and the product of the J_{sc} and V_{oc}. Dividing the product of the V_{oc}, J_{sc}, and FF by the total power of the incident light gives the device efficiency (η_{eff}).

Ideally, this interface between the light absorbing (generally the electron donating phase) and electron accepting phase should be patterned on the length scale set by exciton diffusion lifetimes, typically ~10 nm.[67] Following dissociation, the electron must be transferred through the accepting phase to the cathode and the hole through the donating phase to the anode. This generally requires cocontinuous pathways of each component toward the appropriate electrode. It is not obvious what the exact pattern and morphology of the donor−acceptor interface should be in terms of scale and geometry, but it is clear that the optimization of device performance will rely on the tuning of this architecture.

The efficiency of a photovoltaic device is defined as the ratio of the maximum power produced to the power of the incident radiation (eq 1). This is calculated from a simple current density (J) versus voltage curve generated under standard illumination conditions, as illustrated in Figure 4. From this graph the open-circuit voltage (V_{oc}), short-circuit current density (J_{sc}), and fill factor (FF) of the device are extracted. The efficiency of the device is then calculated as the ratio of the current density and

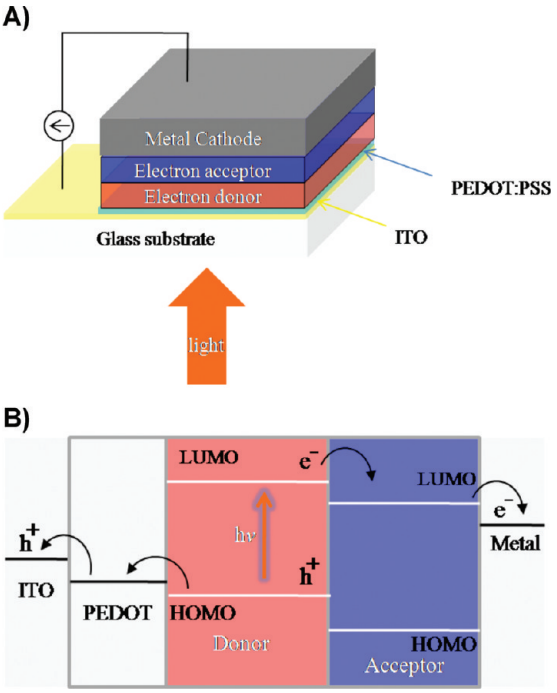

Figure 5. (A) Schematic representation and (B) energy level diagram depicting the basic processes occurring in a simple bilayer donor/acceptor photovoltaic device.

voltage at the point of maximum power (mpp) to the incident illumination power:

$$\eta_{\text{eff}} = \frac{J_{\text{sc}} V_{\text{oc}} \text{FF}}{P_{\text{in}}} = \frac{J_{\text{mpp}} V_{\text{mpp}}}{P_{\text{in}}} \quad (1)$$

The simplest donor−acceptor-based organic photovoltaic device consists of a bilayer comprised of two semiconductors with different energy level alignments sandwiched between a transparent anode (e.g., ITO) for hole collection and a low work function cathode (e.g., Al, Ca, or LiF) for electron collection, as shown in Figure 5. The work function contrast in the electrodes establishes both an internal electric field and carrier gradients, crucial features for establishing asymmetric electron and hole currents. A larger difference between the energy levels of the contacts increases the driving force for charge separation and increases the open-circuit voltage and efficiency of the device.[68,69] As illustrated in Figure 5b, as light is absorbed by the donor, an electron is excited from the HOMO level to the LUMO level, leaving behind a hole. Because of the strong Coulombic interaction between them, the electron and hole form a strongly bound exciton. If the exciton encounters a donor−acceptor interface prior to recombination, the electron in the excited state of the donor will transfer into the LUMO of the acceptor. This charge separation pathway requires that the donor have both a higher LUMO level and HOMO level, creating a molecular analogue to standard semiconductor photovoltaic action at a type II p−n junction. This charge transfer event results in free electrons in the acceptor and free holes in the donor, and both charge carriers are subsequently transferred toward the appropriate electrodes by a hopping mechanism. The first bilayer device of this type consisted of evaporated copper phthalocyanine (donor) and a perylene tetracarboxylic derivative (acceptor) and demonstrated power conversion efficiency of ~1% with large fill factors (~0.65) under simulated air mass 2.0 (AM 2) illumination conditions.[68] This device morphology clearly leads to efficient charge transfer to the electrodes but has minimal donor−acceptor interfacial area. Furthermore, this architecture is most easily implemented with small molecules (as opposed to polymers), which must be evaporated in a costly and sequential fashion.

Increased interfacial area for charge separation can most easily be achieved by blending together the two components in a common solvent and relying on phase separation during casting of the film to create the donor−acceptor interface. This is generally referred to as the bulk heterojunction morphology. Bulk heterojunction devices have been realized in the form of blends consisting of two conjugated polymers[70] or a conjugated polymer with solubilized C_{60} derivatives.[1] The morphologies resulting from phase separation are microscopically irregular, subject to Ostwald ripening, and necessarily difficult to tune in terms of connectivity to the electrodes.[71,72] Significant work has been done on tailoring solvents, wetting interactions, miscibility, and annealing conditions to gain greater control over the length scale and continuity of the phases to the electrodes.[39−42,71,73−78] While some of the highest efficiencies to date have been demonstrated in bulk heterojunction devices, optimization generally requires time-consuming combinatorial processing to achieve optimal morphologies.[53,79,80] Indeed, studies of the relationship between morphologies in blend structures and photovoltaic performance have only begun to appear in the past few years.[67,81−85] Even when a two-component blend is phase-separated, the phases formed will not necessarily be pure components.[86,87] This implies that some degree of mixing at the molecular level will occur and may have complex and unexpected effects on electronic properties of the mixed layer.[88] This is particularly troublesome, as the upper bound on the open-circuit voltage for a device results from the HOMO−LUMO offset across the donor−acceptor interface. Molecular mixing at this interface may indeed be one reason why most OPV devices measured to date have open-circuit voltage potentials much lower than expected from their HOMO−LUMO offsets. Other evidence for the impact of interfacial morphology on device performance comes from studies that annealing procedures and formation of charge transfer states decisively impact device performance. Changes in these charge transfer states, identified through spectroscopy, have been directly correlated to the observed changes in the measured open-circuit potential.[89−91] Additionally, optimization of device contacts is crucial, as band bending near the electrodes has also been shown to reduce the open-circuit potential in several systems.[92,93] In short, it is clear that a well-defined and controllable interface between the donor and acceptor is required in order to optimize the performance of organic photovoltaic devices.

The level of control necessary to nanostructure donor−acceptor interfaces with molecularly pure phases can potentially be realized through donor−acceptor diblock copolymers. Not only does self-assembly lead to regularly sized and spaced nanodomains ideal for charge separation, molecular scale mixing is confined to only interfacial broadening[94,95] and may lead to a much enhanced ability to control energy levels and exciton separation. The ideal morphologies for photovoltaic cells, however, may require aligned nanostructures to more precisely control charge transport. As mentioned previously, similar types of alignment strategies have already been developed for block copolymer lithographic applications.

The synthesis of bipolar block copolymers for these applications requires a combination of routes in order to achieve both the desired functionality and control over polydispersity and chain length. While it has been well demonstrated that classical coil-shaped block copolymers are remarkably tolerant of polydispersity,[96] polydispersity in the fully extended rod block translates directly into interfacial broadening due to the rod's inability to reconform.[97] The Hadziioannou group has prepared a number of bipolar donor−acceptor block copolymers by using

an electron donating poly(alkoxyphenylenevinylene) (PPV) rod as the macroinitiator for the living free radical growth of a coil. The PPV rod has relatively low polydispersity (PDI ~ 1.3) due to a self-limiting polymerization via a Siegrist condensation. Following the living free radical growth of the coil block, fullerenes are then attached pendant to the coil.[53,98−101] These materials demonstrate improved solar cell device performance in block copolymers as opposed to analogous blends of the constituent homopolymers, though self-assembly was significantly hindered by the presence of the bulky fullerenes.[53,101] A similar fullerene containing block copolymer, in which the PPV has been replaced with P3HT, demonstrates similar behavior.[102,103] Sun and co-workers designed a donor−bridge−acceptor−bridge (DBAB) type block copolymer to minimize the exciton recombination and carrier losses.[104−108] Similarly, Scherf and co-workers prepared a series of diblock/triblock copolymers with both electron donor and electron acceptor blocks, which exhibit the formation of regular nanosize mesostructures in thin film state.[56,57,109] Thelakkat and co-workers have fabricated a novel coil−coil donor−acceptor block copolymer poly(bisphenyl-4-vinylphenylamine-*block*-perylene diimide acrylate) in which all of the electronic functionalities are attached as side groups.[79,110−113]

Poly(3-hexylthiophene) (P3HT) is an attractive choice as the electron donating block due to its relatively high charge carrier mobilities (maximum ~0.1 $cm^2\ V^{-1}\ s^{-1}$), ease of synthesis with low polydispersity, and controlled molecular weights.[114,115] Boudouris et al. have demonstrated the self-assembly of a P3HT block copolymer in which the coil block, poly(lactic acid), may be easily decomposed and backfilled with PCBM. In this case, block copolymer self-assembly is used simply to pattern the P3HT into a nanoporous network rather than directly fabricating the donor−acceptor interface.[116] Recently, block copolymers incorporating P3HT as the donor material and a hybrid acceptor material made of an acrylate backbone with pendant perylene groups have been synthesized by several groups.[103,117−119] This block copolymer system has shown improved device performance in comparison to an analogous blend, suggesting that the molecular scale phase separation of a block copolymer is advantageous, but its steric bulk poses a challenge to controllable self-assembly. The stabilization of blend morphologies against ripening through the use of block copolymer surfactants has also been used to improve performance in P3HT/[6,6]-phenyl-C_{61}-butyric acid methyl ester (PCBM) blend photovoltaics.[120]

Block Copolymers for Organic Light Emitting Diodes (OLEDs)

The simplest embodiment of an organic light emitting diode (OLED) consists of several layers of active material placed between a low work function cathode and a transparent anode. Electrons and holes are injected from the electrodes, drift through the field, and then recombine as excitons, which may radiatively decay to produce photons. The external quantum efficiency (η_{ext}), therefore, relies on the optimization of each of the above steps and can be expressed as

$$\eta_{ext} = \gamma r_{st} q \eta_{coupling} \quad (2)$$

where γ refers to the ratio of electrons to holes, r_{st} is the ratio of singlet to triplet excitons formed from these charges, q refers to the nonradiative decay pathways for excitonic emission, and $\eta_{coupling}$ accounts for the fraction of light generated in the device that is unable to escape.[121] Not only do electrons and holes have vastly different injection efficiencies from the most common electrodes, which disturbs charge balance, they possess very different field effect mobilities in most organic semiconductors.

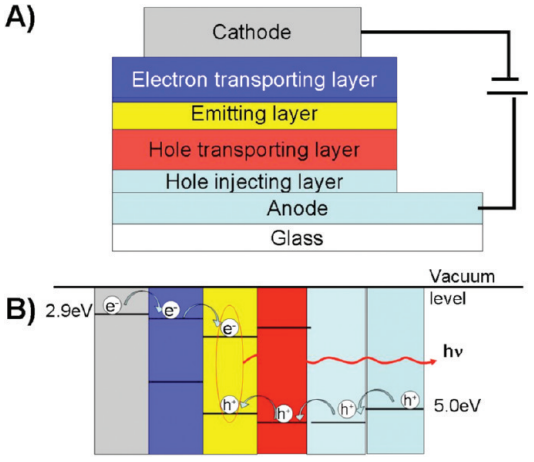

Figure 6. Organic light emitting diodes (OLEDs) are generally fabricated from multiple components meant to balance charge transport and manage recombination/emission events (A) and matching energy level diagram (B). The cathode is generally a low work function metal (e.g., Ca or Mg) while the anode is generally transparent to allow light to exit. Indium tin oxide (ITO) is a common choice.

As a result, high efficiency devices consist of multiple layers so as to separately optimize each step,[122] as shown in Figure 6. The layers are used to balance the number of electrons and holes injected and manage their transport to optimize γ. When the charges recombine, they may form two types of excitons: singlets (25%) have a radiative decay pathway and triplets (75%) that decay through nonradiative processes. Most organics are incapable of singlet−triplet coupling so as a result only 25% of the excitons are available for emission. Frequently, phosphors are included in the emitting layer to correct for this problem.[123]

The multilayered scheme shown in Figure 6 is most easily realized in small molecule organics, which are commonly evaporated sequentially to form multiple layers. These layered devices are now approaching the theoretical limits of quantum efficiency[124] and are in commercial production. Though several processing techniques and device architectures which allow for large area devices from small molecule evaporated components have been developed,[125−127] solution processing offers advantages in terms of expense and ease of implementation. Simple blending of the components provides an easier processing route but also tends to result in both molecular scale mixing, which has unfavorable effects on electronic properties, and a strong dependence on morphology, which is difficult to control.[76] The sequential deposition of polymeric layers combines both the advantages of solution processing with the ideal morphology from small molecule OLEDs. This route presents a processing challenge since sequential layers must have orthogonal solubility properties (so that lower layers are not dissolved in subsequent processing steps). Much work has focused on solvent matching, cross-linking, and other processing techniques to facilitate subsequent layer deposition.[128−139]

Block copolymers, alternatively, allow for the incorporation of both electron and hole transporting moieties in a single solution-processing step. Further, the ability to pattern on a ~10 nm length scale may result in appropriate morphologies for the reduction of charge injection barriers and quenching at the electrodes while facilitating charge transport and recombination at the block copolymer interfaces. Many groups are pursuing the chemistry necessary to incorporate both electron and hole transporting moieties onto a single polymeric chain.[140−145] Furthermore, the incorportion of multiple luminescent moieties onto a single backbone is a route toward color tunability, primarily white light emission. Kim et al. have prepared a new

class of silicon-containing poly(cyanoterephthalylidene) copolymers by incorporating electron-withdrawing cyano groups into the π-conjugated systems.[146] Random copolymers based on poly(9,9-di-*n*-hexylfluorene-*co*-anthracene) (DHF−ANT) incorporate both hole transporting triphenylamine (TPA) and electron transporting oxadiazole (OX) components to achieve charge balanced devices.[143] Double-layer devices including a layer of the random copolymer and a separate hole transporting crosslinked TPA layer demonstrated device efficiencies an order of magnitude higher than single-layer devices due to the improved charge injection and charge recombination. Similarly, incorporating the electron transport moieties (OX) as side chains on luminescent, hole-transporting poly(phenylenevinylene) derivates increased device performance due principally to the balancing of charge injection and transport.[147,148] This strategy may also be implemented by incorporating hole transporting carbazole moieties into well-defined polyfluorenes (PF).[149] Xiao et al. prepared a series of conjugated triblock copolymers containing hole-transporting polycarbazole segments, electron-transporting polyoxadiazole segments, and blue light-emitting polyfluorene segments synthesized by Suzuki polycondensation methods.[150]

As mentioned above, spin statistics commonly limit emission in organics to ~25% of the overall population of excitons created upon charge recombination. However, this may be bypassed through incorporation of a heavy metal center, such as platinum- or iridium-containing compounds, which introduce spin−orbit coupling and enable phosphorescence and higher emission efficiencies.[151] Phosphors are frequently used as emission layers within layered small molecule OLEDs. Frechét, Thompson, and co-workers demonstrated this concept in solution-processed polymeric systems by synthesizing platinum-functionalized phosphorescent random copolymers, containing electron (OX) and hole (TPA) transporting moieties as side chains on a nonconjugated backbone. This resulted in solution-processable, efficient, and near-white-light organic light emitting diodes, as shown in Figure 7.[152,153] Further studies have shown that single-layer polymer light emitting diodes from block copolymers have better device performance than random copolymers due to the nanostructuring of the block copolymers which lowered charge transport barriers and facilitated electron−hole recombination.[142] Conjugated block polymers are also attractive choices for OLED applications, though less work has been done on these systems. Poly(alkoxyphenylenevinylenes) can be joined with OX blocks to create block copolymers with one conjugated hole transporting, emissive block and one electron transporting, nonconjugated block. As cast, these films form nanoscale lamellae in grains running both parallel and perpendicular to the substrate. In this case, block copolymer self-assembly leads to nanoscale structuring and improvements in OLED efficiency as compared to an analogous blend.[154] One avenue for significant improvement is control over the orientation of the recombination interface in all of the above-mentioned block copolymer systems. It is not yet clear whether interfaces running parallel to the substrate or perpendicular from it will optimally balance the processes of charge transport versus recombination.

Studies on bipolar block copolymers indicate that the nanophase segregation of components (as opposed to the mixing inherent in random copolymers) is advantageous to OLED performance.[142,154] Additionally, backbone conjugation generally imparts higher charge mobility. A block copolymer strategy employing luminescent conjugated polymers, however, presents major hurdles in terms of synthetic limitations and hindered self-assembly. Designed nanoscale morphological control requires well-defined block copolymers with controllable molecular weight and narrow polydispersity. Most conjugated polymers are made via condensation routes and are highly polydisperse, though a few routes exist toward molecular weight and polydispersity

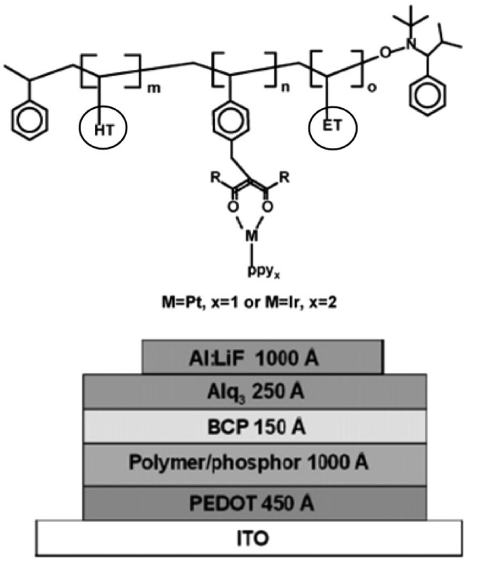

Figure 7. Block copolymers can be used to mimic the multilayer structures successful in small molecule OLEDs. In this case Deng et al. use a block copolymer consisting of a hole transporting block (HT, containing triphenylamine pendant groups), an electron transporting block (ET, containing oxadiazole pendant groups), and a phosphorescent block. Reprinted with permission from ref 153.

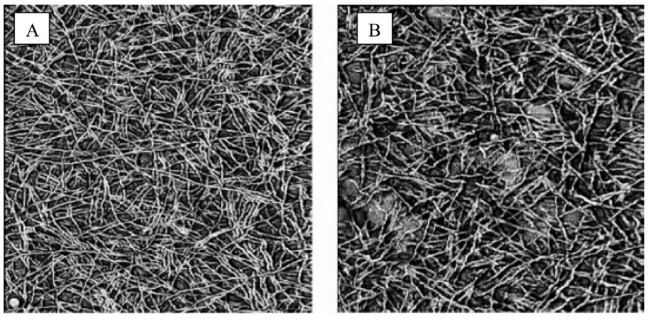

Figure 8. P3HT has a very distinct crystalline fibrillar structure (A) which appears to dominate over block copolymer self-assembly such that a P3HT-*b*-polystyrene block copolymer (B) appears to have a nearly identical nanostructure. Reprinted with permission from ref 159. Copyright 2006 Taylor and Francis.

control.[155−158] In addition, conjugated polymers, as previously discussed, tend to have rigid backbones, and their self-assembly is fundamentally different than classical block copolymer systems. As a result, most of the above work focused on polymers with pendant electron conducting, hole conducting, or luminescent moieties.

Outlook

Over the past several years, there have been significant developments both in the synthesis of block copolymers for organic electronics and in the understanding of how conjugation and electrical functionality affect self-assembly. The principal advantage inherent to organic electronics (in addition to much discussed processability and cost) is an ability to tune the optical band gap as well as the electronic energy levels via synthetic chemistry. Similarly, the advantage of block copolymers lies in an inherent control over nanostructure which is based on chemical structure (length of chain, block fraction, etc.). Combining electronic functionality with control over morphology on a length scale relevant for charge separation, recombination, and transport makes these semiconducting block copolymers promising candidates for high-performance optoelectronic devices. The fact

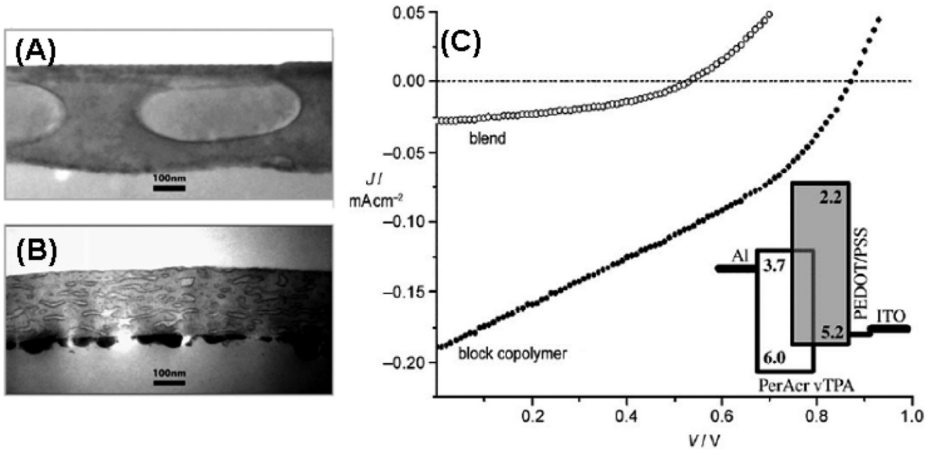

Figure 9. Cross-sectional TEM images of a thin film of (A) a blend of PPerAcr and PvTPA and (B) a block copolymer of PerAcr-*b*-PvTPA showing that the block copolymers yield devices with smaller domain sizes. Device data (C) show that the block copolymer gives significantly better performance which is associated with decreased domain sizes, increased interfacial area, and increased connectivity of the films improving charge separation and transport. Reproduced with permission from ref 79. Copyright 2006 Wiley-VCH Verlag GmbH & Co. KGaA.

that block copolymer photovoltaics are promising when compared to *analogous* blends but are universally reporting efficiencies far less than those of the *best* bulk heterojunction cells indicates that there remains a long way to go in realizing this potential. There are significant gaps in our ability to make use of the block copolymer strategy in nanostructured organic electronics, ranging from fundamental understanding of self-assembly and pattern control to chemical synthesis.

Much of this promise relies on the beauty of classical block copolymer self-assembly, which collapses onto a single phase diagram characterized by volume fraction (ϕ) and the Flory−Huggins segregation strength (χN), regardless of the specific chemistry of each block. Work on conjugated rod−coil block copolymers suggests a single phase diagram which is parametrized by ϕ, ν, χN, μN, and ratios of the last two parameters. A majority of this fundamental experimental work has focused on poly(phenylenevinylene) block copolymers, and the universality of this phase diagram has not yet been thoroughly tested. In fact, it is quite clear that lower bandgap polymers must be developed in order to achieve higher power conversion efficiencies[80] and, similarly, materials with phosphorescence ability or more carefully tuned emission wavelengths are necessary for organic light emitting diodes. In addition to the clear challenges of incorporating these new chemistries into facile routes toward block copolymer synthesis, we must understand their role in self-assembly. For example, P3HT appears to be much more suitable for photovoltaic performance but has much higher melting temperatures such that crystallization will necessarily compete with self-assembly. It is unsurprising therefore that P3HT-containing block copolymers demonstrate a fibrillar structure which may result from crystallization,[114,159,160] as shown in Figure 8. Similarly, perylene diimide is a promising electron acceptor attached pendant to a polymer chain; however, it is known to π stack very strongly.[161] These intramolecular interactions are sure to strongly affect domain shape, size, continuity, and orientation all of which will have unexpected consequences on device performance.

While several donor−acceptor and electron−hole transporting block copolymers have been demonstrated, well-organized nanostructures have been slow to appear. In particular, the degree of order in block copolymers can be controlled by modulating chain mobility and the amount of time that the polymer is free to self-assemble. If cast quickly from a nonpreferential solvent, the film can be trapped in a molecularly mixed state. If annealed or plasticized to allow for molecular motion, the system may gain the longer range order typical of classical block copolymers. Intermediate conditions may lead to well-defined interfaces with only short-range order. It is not immediately clear which of these three scenarios is best from a device efficiency standpoint. While historically long-range order has been a goal for most block copolymer systems, in this case short-range order lends the appropriate degree of nanodomain purity, and the lack of long-range order leads to more interconnectivity between domains and perhaps better transport. Clearly optimizing the necessary degree of long-range order and understanding the role of morphological defects on electronic properties and device efficiency are crucial parameters in the design of block copolymer optoelectronic films. While preliminary photovoltaic device structures made from the aforementioned block copolymers demonstrate promising short-circuit currents and open-circuit voltages, as shown in Figure 9, optimization of device efficiency relies on the use of carefully constructed nanostructures to probe the effects on device performance.

For example, the phase diagram of semiconducting rod−coil block copolymers suggests that lamellae form across a large portion of phase space, so it is possible to alter the fraction of hole transporter versus electron transporter in block copolymers for OLEDs while maintaining the same morphology. This sort of study will allow for the independent investigation of the roles of charge balancing and nanostructuring. Similarly, by comparing devices frozen in the lamellar, nematic, and isotropic phases, an understanding of how rod arrangement and nanodomain morphology *each* impact device performance may emerge. Further, in poly(phenylenevinylene) (PPV) rod−coil polymers, as the PPV rods self-assemble on one side of an interface, they align with a higher degree of order than in the homopolymer,[7,28] which implies a larger degree of packing among rods and perhaps greater interchain electrical hopping in the block copolymer than homopolymer.[128,162] The nanodomain orientation also clearly affects charge transport pathways and the accessibility of the internal interfaces. Alignment of these rigid and strongly crystalline conjugated molecules is a challenge since they have such low inherent chain mobility compared to traditional block copolymers. Confinement issues in a thin film are also likely exacerbated when dealing with rigid molecules. On the other hand, the presence of a liquid crystalline block suggests the availability of a whole new class of alignment techniques previously developed for liquid crystals (such as magnetic field alignment and surface rubbing) that have not been effective on classical block copolymers.

Conclusions

Block copolymer strategies may be very promising in optimizing optoelectronic device performance by controlling the morphology of the active layer on the same length scale as an exciton diffusion length while also providing optimized morphologies for charge transport. As discussed within this Perspective, many strategies have been suggested for both the synthesis of block copolymers containing multiple electronically interesting components and control over their self-assembly. Much work is still necessary to prove the utility of block copolymers in this arena through (among other topics) the patterning of interfaces through controlled self-assembly and a much more detailed understanding of the role of detailed morphology on device behavior.

Acknowledgment. We gratefully acknowledge support from the DOE-BES Plastic Electronics Program at Lawrence Berkeley National Laboratories. J.J.U. acknowledges additional support from the DOE-BES Molecular Foundry at Lawrence Berkeley National Laboratories under Contract DE-AC02-05CH11231. S.K. gratefully acknowledges a postdoctoral fellowship for energy research from the Technion Israel Institute of Technology.

References and Notes

(1) Yu, G.; Gao, J.; Hummelen, J. C.; Wudl, F.; Heeger, A. J. *Science* **1995**, *270* (5243), 1789–1791.
(2) Greenham, N. C.; Moratti, S. C.; Bradley, D. D. C.; Friend, R. H.; Holmes, A. B. *Nature* **1993**, *365* (6447), 628–630.
(3) Bates, F. S.; Fredrickson, G. H. *Phys. Today* **1999**, *52* (2), 32–38.
(4) Segalman, R. A. *Mater. Sci. Eng., R* **2005**, *48* (3), 191–226.
(5) Su, W. P.; Schrieffer, J. R.; Heeger, A. J. *Phys. Rev. B* **1980**, *22* (4), 2099.
(6) Hoegl, H. *J. Phys. Chem.* **1965**, *69* (3), 755–766.
(7) Olsen, B. D.; Jang, S. Y.; Luning, J. M.; Segalman, R. A. *Macromolecules* **2006**, *39* (13), 4469–4479.
(8) Chen, J. T.; Thomas, E. L.; Ober, C. K.; Hwang, S. S. *Macromolecules* **1995**, *28* (5), 1688–1697.
(9) Chen, J. T.; Thomas, E. L.; Ober, C. K.; Mao, G. P. *Science* **1996**, *273* (5273), 343–346.
(10) Lee, M.; Cho, B. K.; Zin, W. C. *Chem. Rev.* **2001**, *101* (12), 3869–3892.
(11) Li, C. Y.; Tenneti, K. K.; Zhang, D.; Zhang, H. L.; Wan, X. H.; Chen, E. Q.; Zhou, Q. F.; Carlos, A. O.; Igos, S.; Hsiao, B. S. *Macromolecules* **2004**, *37* (8), 2854–2860.
(12) Radzilowski, L. H.; Carragher, B. O.; Stupp, S. I. *Macromolecules* **1997**, *30* (7), 2110–2119.
(13) Olsen, B. D.; Segalman, R. A. *Mater. Sci. Eng., R* **2008**, *62* (2), 37–66.
(14) Hamley, I. W. *The Physics of Block Copolymers*; Oxford University Press: New York, 1998.
(15) Semenov, A. N. *Mol. Cryst. Liq. Cryst.* **1991**, *209*, 191–199.
(16) Semenov, A. N.; Vasilenko, S. V. *Zh. Eksp. Teor. Fiz.* **1986**, *90* (1), 124–140.
(17) Halperin, A. *Europhys. Lett.* **1989**, *10* (6), 549–553.
(18) Halperin, A. *Macromolecules* **1990**, *23* (10), 2724–2731.
(19) Williams, D. R. M.; Fredrickson, G. H. *Macromolecules* **1992**, *25* (13), 3561–3568.
(20) Holyst, R.; Schick, M. *J. Chem. Phys.* **1992**, *96* (1), 730–740.
(21) Singh, C.; Goulian, M.; Liu, A. J.; Fredrickson, G. H. *Macromolecules* **1994**, *27* (11), 2974–2986.
(22) Reenders, M.; ten Brinke, G. *Macromolecules* **2002**, *35* (8), 3266–3280.
(23) Brinkmann, M.; Chan, V. Z. H.; Thomas, E. L.; Lee, V. Y.; Miller, R. D.; Hadjichristidis, N.; Avgeropoulos, A. *Chem. Mater.* **2001**, *13* (3), 967–972.
(24) Hulvat, J. F.; Sofos, M.; Tajima, K.; Stupp, S. I. *J. Am. Chem. Soc.* **2005**, *127* (1), 366–372.
(25) Radzilowski, L. H.; Stupp, S. I. *Macromolecules* **1994**, *27* (26), 7747–7753.
(26) Olsen, B. D.; Segalman, R. A. *Macromolecules* **2005**, *38* (24), 10127–10137.
(27) Olsen, B. D.; Segalman, R. A. *Macromolecules* **2006**, *39* (20), 7078–7083.
(28) Olsen, B. D.; Segalman, R. A. *Macromolecules* **2007**, *40* (19), 6922–6929.
(29) Olsen, B. D.; Shah, M.; Ganesan, V.; Segalman, R. A. *Macromolecules* **2008**, *41* (18), 6809–6817.
(30) Sary, N.; Rubatat, L.; Brochon, C.; Hadziioannou, G.; Ruokolainen, J.; Mezzenga, R. *Macromolecules* **2007**, *40*, 6990–6997.
(31) Sary, N.; Mezzenga, R.; Brochon, C.; Hadziioannou, G.; Ruokolainen, J. *Macromolecules* **2007**, *40* (9), 3277–3286.
(32) Sary, N.; Brochon, C.; Hadziioannou, G.; Mezzenga, R. *Eur. Phys. J. E* **2007**, *24* (4), 379–384.
(33) Sary, N.; Rubatat, L.; Brochon, C.; Hadziioannou, G.; Ruokolainen, J.; Mezzenga, R. *Macromolecules* **2007**, *40* (19), 6990–6997.
(34) Ho, C.-C.; Lee, Y.-H.; Dai, C.-A.; Segalman, R. A.; Su, W.-F. *Macromolecules* **2009**, *42* (12), 4208−4219.
(35) Dai, C. A.; Yen, W. C.; Lee, Y. H.; Ho, C. C.; Su, W. F. *J. Am. Chem. Soc.* **2007**, *129* (36), 11036–11038.
(36) Lee, M.; Cho, B. K.; Oh, N. K.; Zin, W. C. *Macromolecules* **2001**, *34* (6), 1987–1995.
(37) Pryamitsyn, V.; Ganesan, V. *J. Chem. Phys.* **2004**, *120* (12), 5824–5838.
(38) Matsen, M. W.; Barrett, C. *J. Chem. Phys.* **1998**, *109* (10), 4108–4118.
(39) Olsen, B. D.; Li, X. F.; Wang, J.; Segalman, R. A. *Macromolecules* **2007**, *40* (9), 3287–3295.
(40) Olsen, B. D.; Alcazar, D.; Krikorian, V.; Toney, M. F.; Thomas, E. L.; Segalman, R. A. *Macromolecules* **2008**, *41* (1), 58–66.
(41) Olsen, B. D.; Toney, M. F.; Segalman, R. A. *Langmuir* **2008**, *24* (5), 1604–1607.
(42) Olsen, B. D.; Li, X. F.; Wang, J.; Segalman, R. A. *Soft Matter* **2009**, *5* (1), 182–192.
(43) Hamley, I. W. *Nanotechnology* **2003**, *14* (10), R39–R54.
(44) Lazzari, M.; Lopez-Quintela, M. A. *Adv. Mater.* **2003**, *15* (19), 1583–1594.
(45) Park, C.; Yoon, J.; Thomas, E. L. *Polymer* **2003**, *44* (22), 6725–6760.
(46) Morkved, T. L.; Lu, M.; Urbas, A. M.; Ehrichs, E. E.; Jaeger, H. M.; Mansky, P.; Russell, T. P. *Science* **1996**, *273* (5277), 931–933.
(47) Tao, Y.; Zohar, H.; Olsen, B. D.; Segalman, R. A. *Nano Lett.* **2007**, *7* (9), 2742–2746.
(48) Grell, M.; Bradley, D. D. C. *Adv. Mater.* **1999**, *11* (11), 895–905.
(49) Tu, G. L.; Li, H. B.; Forster, M.; Heiderhoff, R.; Balk, L. J.; Sigel, R.; Scherf, U. *Small* **2007**, *3* (6), 1001–1006.
(50) Scherf, U.; Gutacker, A.; Koenen, N. *Acc. Chem. Res.* **2008**, *41* (9), 1086–1097.
(51) Bolognesi, A.; Betti, P.; Botta, C.; Destri, S.; Giovanella, U.; Moreau, J.; Pasini, M.; Porzio, W. *Macromolecules* **2009**, *42* (4), 1107–1113.
(52) Yang, C.; Lee, J. K.; Heeger, A. J.; Wudl, F. *J. Mater. Chem.* **2009**, *19* (30), 5416–5423.
(53) de Boer, B.; Stalmach, U.; van Hutten, P. F.; Melzer, C.; Krasnikov, V. V.; Hadziioannou, G. *Polymer* **2001**, *42* (21), 9097–9109.
(54) Leclère, P.; Hennebicq, E.; Calderone, A.; Brocorens, P.; Grimsdale, A. C.; Müllen, K.; Brédas, J. L.; Lazzaroni, R. *Prog. Polym. Sci.* **2003**, *28* (1), 55–81.
(55) Lu, S.; Liu, T.; Ke, L.; Ma, D.-G.; Chua, S.-J.; Huang, W. *Macromolecules* **2005**, *38* (20), 8494–8502.
(56) Asawapirom, U.; Guntner, R.; Forster, M.; Scherf, U. *Thin Solid Films* **2005**, *477* (1−2), 48–52.
(57) Guntner, R.; Asawapirom, U.; Forster, M.; Schmitt, C.; Stiller, B.; Tiersch, B.; Falcou, A.; Nothofer, H. G.; Scherf, U. *Thin Solid Films* **2002**, *417* (1−2), 1–6.
(58) Liping, H.; Jin, Z.; Yong, Z.; Jinjie, X.; Xianliang, S.; Lei, J. *ChemPhysChem* **2006**, *7* (12), 2520–2525.
(59) Stalmach, U.; de Boer, B.; Videlot, C.; van Hutten, P. F.; Hadziioannou, G. *J. Am. Chem. Soc.* **2000**, *122* (23), 5464–5472.
(60) Huo, H.; Li, K.; Wang, Q.; Wu, C. *Macromolecules* **2007**, *40* (18), 6692–6698.
(61) Schenning, A. P. H. J.; Kilbinger, A. F. M.; Biscarini, F.; Cavallini, M.; Cooper, H. J.; Derrick, P. J.; Feast, W. J.; Lazzaroni, R.; Leclere, P.; McDonell, L. A.; Meijer, E. W.; Meskers, S. C. J. *J. Am. Chem. Soc.* **2002**, *124* (7), 1269–1275.

(62) Kim, H. J.; Jung, E. Y.; Jin, L. Y.; Lee, M. *Macromolecules* **2008**, *41* (16), 6066–6072.
(63) Jenekhe, S. A.; Chen, X. L. *Science* **1999**, *283* (5400), 372–375.
(64) Sariciftci, N. S.; Smilowitz, L.; Heeger, A. J.; Wudl, F. *Science* **1992**, *258* (5087), 1474–1476.
(65) Heeger, A. J. *Rev. Mod. Phys.* **2001**, *73* (3), 681–700.
(66) Bredas, J. L.; Cornil, J.; Heeger, A. J. *Adv. Mater.* **1996**, *8* (5), 447–452.
(67) Hoppe, H.; Sariciftci, N. S. *J. Mater. Chem.* **2006**, *16* (1), 45–61.
(68) Tang, C. W. *Appl. Phys. Lett.* **1986**, *48* (2), 183–185.
(69) Peumans, P.; Yakimov, A.; Forrest, S. R. *J. Appl. Phys.* **2003**, *93* (7), 3693–3723.
(70) Yu, G.; Heeger, A. J. *J. Appl. Phys.* **1995**, *78* (7), 4510–4515.
(71) Arias, A. C.; MacKenzie, J. D.; Stevenson, R.; Halls, J. J. M.; Inbasekaran, M.; Woo, E. P.; Richards, D.; Friend, R. H. *Macromolecules* **2001**, *34* (17), 6005–6013.
(72) Kim, Y.; Cook, S.; Choulis, S. A.; Nelson, J.; Durrant, J. R.; Bradley, D. D. C. *Chem. Mater.* **2004**, *16* (23), 4812–4818.
(73) Thompson, B. C.; Frechet, J. M. J. *Angew. Chem., Int. Ed.* **2008**, *47* (1), 58–77.
(74) Arias, A. C.; Corcoran, N.; Banach, M.; Friend, R. H.; MacKenzie, J. D.; Huck, W. T. S. *Appl. Phys. Lett.* **2002**, *80* (10), 1695–1697.
(75) Chappell, J.; Lidzey, D. G.; Jukes, P. C.; Higgins, A. M.; Thompson, R. L.; O'Connor, S.; Grizzi, I.; Fletcher, R.; O'Brien, J.; Geoghegan, M.; Jones, R. A. L. *Nat. Mater.* **2003**, *2* (9), 616–621.
(76) Moons, E. *J. Phys.: Condens. Matter* **2002**, *14* (47), 12235–12260.
(77) Zhang, F. L.; Jespersen, K. G.; Bjorstrom, C.; Svensson, M.; Andersson, M. R.; Sundstrom, V.; Magnusson, K.; Moons, E.; Yartsev, A.; Inganas, O. *Adv. Funct. Mater.* **2006**, *16* (5), 667–674.
(78) Bertho, S.; Haeldermans, I.; Swinnen, A.; Moons, W.; Martens, T.; Lutsen, L.; Vanderzande, D.; Manca, J.; Senes, A.; Bonfiglio, A. *Sol. Energy Mater. Sol. Cells* **2007**, *91* (5), 385–389.
(79) Lindner, S. M.; Huttner, S.; Chiche, A.; Thelakkat, M.; Krausch, G. *Angew. Chem., Int. Ed.* **2006**, *45* (20), 3364–3368.
(80) Park, S. H.; Roy, A.; Beaupre, S.; Cho, S.; Coates, N.; Moon, J. S.; Moses, D.; Leclerc, M.; Lee, K.; Heeger, A. J. *Nat. Photonics* **2009**, *3* (69), 297.
(81) Shaheen, S. E.; Brabec, C. J.; Sariciftci, N. S.; Padinger, F.; Fromherz, T.; Hummelen, J. C. *Appl. Phys. Lett.* **2001**, *78* (6), 841–843.
(82) Chirvase, D.; Parisi, J.; Hummelen, J. C.; Dyakonov, V. *Nanotechnology* **2004**, *15* (9), 1317–1323.
(83) Hoppe, H.; Niggemann, M.; Winder, C.; Kraut, J.; Hiesgen, R.; Hinsch, A.; Meissner, D.; Sariciftci, N. S. *Adv. Funct. Mater.* **2004**, *14* (10), 1005–1011.
(84) Yang, S.; Chen, G.; Megens, M.; Ullal, C. K.; Han, Y. J.; Rapaport, R.; Thomas, E. L.; Aizenberg, J. *Adv. Mater.* **2005**, *17* (4), 435−438.
(85) Yang, X. N.; Loos, J.; Veenstra, S. C.; Verhees, W. J. H.; Wienk, M. M.; Kroon, J. M.; Michels, M. A. J.; Janssen, R. A. J. *Nano Lett.* **2005**, *5* (4), 579–583.
(86) Helfand, E.; Tagami, Y. *J. Chem. Phys.* **1972**, *57* (4), 1812–1813.
(87) Helfand, E.; Tagami, Y. *J. Chem. Phys.* **1972**, *56* (7), 3592–3601.
(88) Bull, T. A.; Pingree, L. S. C.; Jenekhe, S. A.; Ginger, D. S.; Luscombe, C. K. *ACS Nano* **2009**, *3* (3), 627–636.
(89) Goris, L.; Haenen, K.; Nesladek, M.; Wagner, P.; Vanderzande, D.; De Schepper, L.; D'Haen, J.; Lutsen, L.; Manca, J. V. *J. Mater. Sci.* **2005**, *40* (6), 1413–1418.
(90) Vandewal, K.; Gadisa, A.; Oosterbaan, W. D.; Bertho, S.; Banishoeib, F.; Van Severen, I.; Lutsen, L.; Cleij, T. J.; Vanderzande, D.; Manca, J. V. *Adv. Funct. Mater.* **2008**, *18* (14), 2064–2070.
(91) Haeldermans, I.; Vandewal, K.; Oosterbaan, W. D.; Gadisa, A.; D'Haen, J.; Van Bael, M. K.; Manca, J. V.; Mullens, J. *Appl. Phys. Lett.* **2008**, *93* (22), 223302.
(92) Veldman, D.; Meskers, S. C. J.; Janssen, R. A. J. *Adv. Funct. Mater.* **2009**, *19* (12), 1939−1948.
(93) Simmons, J. G. *J. Phys. Chem. Solids* **1971**, *32* (8), 1987–1999.
(94) Hamley, I. W. *The Physics of Block Copolymers*; Oxford University Press: New York, 1998; p 425.
(95) Bates, F. S.; Fredrickson, G. H. *Annu. Rev. Phys. Chem.* **1990**, *41*, 525–557.
(96) Lynd, N. A.; Meuler, A. J.; Hillmyer, M. A. *Prog. Polym. Sci.* **2008**, *33* (9), 875–893.
(97) Schlaad, H.; Smarsly, B.; Losik, M. *Macromolecules* **2004**, *37* (6), 2210–2214.
(98) van der Veen, M. H.; de Boer, B.; Stalmach, U.; van de wetering, K. I.; Hadziioannou, G. *Macromolecules* **2004**, *37* (10), 3673–3684.
(99) Heiser, T.; Adamopoulos, G.; Brinkmann, M.; Giovanella, U.; Ould-Saad, S.; Brochon, C.; van de Wetering, K.; Hadziioannou, G. *Thin Solid Films* **2006**, *511*, 219–223.
(100) Van De Wetering, K.; Brochon, C.; Ngov, C.; Hadziioannou, G. *Macromolecules* **2006**, *39* (13), 4289–4297.
(101) Barrau, S.; Heiser, T.; Richard, F.; Brochon, C.; Ngov, C.; van de Wetering, K.; Hadziioannou, G.; Anokhin, D. V.; Ivanov, D. A. *Macromolecules* **2008**, *41* (7), 2701–2710.
(102) Lee, J. U.; Cirpan, A.; Emrick, T.; Russell, T. P.; Jo, W. H. *J. Mater. Chem.* **2009**, *19* (10), 1483–1489.
(103) Richard, F.; Brochon, C.; Leclerc, N.; Eckhardt, D.; Heiser, T.; Hadziioannou, G. *Macromol. Rapid Commun.* **2008**, *29* (11), 885–891.
(104) Sun, S. S.; Zhang, C.; Ledbetter, A.; Choi, S.; Seo, K.; Bonner, C. E.; Drees, M.; Sariciftci, N. S. *Appl. Phys. Lett.* **2007**, *90* (4).
(105) Zhang, C.; Choi, S.; Haliburton, J.; Cleveland, T.; Li, R.; Sun, S. S.; Ledbetter, A.; Bonner, C. E. *Macromolecules* **2006**, *39* (13), 4317–4326.
(106) Sun, S. S.; Fan, Z.; Wang, Y. Q.; Winston, K.; Bonner, C. E. *Mater. Sci. Eng., B* **2005**, *116* (3), 279–282.
(107) Sun, S. S. *Mater. Sci. Eng., B* **2005**, *116* (3), 251–256.
(108) Sun, S. S. *Sol. Energy Mater. Sol. Cells* **2003**, *79* (2), 257–264.
(109) Tu, G. L.; Li, H. B.; Forster, M.; Heiderhoff, R.; Balk, L. J.; Scherf, U. *Macromolecules* **2006**, *39* (13), 4327–4331.
(110) Lindner, S. M.; Thelakkat, M. *Macromolecules* **2004**, *37* (24), 8832–8835.
(111) Sommer, M.; Thelakkat, M. *Eur. Phys. J.: Appl. Phys.* **2006**, *36* (3), 245–249.
(112) Lindner, S. M.; Kaufmann, N.; Thelakkat, M. *Org. Electron.* **2007**, *8* (1), 69–75.
(113) Sommer, M.; Lindner, S. M.; Thelakkat, M. *Adv. Funct. Mater.* **2007**, *17* (9), 1493–1500.
(114) Iovu, M. C.; Sheina, E. E.; Gil, R. R.; McCullough, R. D. *Macromolecules* **2005**, *38* (21), 8649–8656.
(115) Sheina, E. E.; Liu, J. S.; Iovu, M. C.; Laird, D. W.; McCullough, R. D. *Macromolecules* **2004**, *37* (10), 3526–3528.
(116) Boudouris, B. W.; Frisbie, C. D.; Hillmyer, M. A. *Macromolecules* **2008**, *41* (1), 67–75.
(117) Sommer, M.; Lang, A. S.; Thelakkat, M. *Angew. Chem., Int. Ed.* **2008**, *47* (41), 7901–7904.
(118) Tao, Y.; McCulloch, B.; Kim, S.; Segalman, R. A. *Soft Matter* **2009**, *5*, 4219−4230.
(119) Zhang, Q. L.; Cirpan, A.; Russell, T. P.; Emrick, T. *Macromolecules* **2009**, *42* (4), 1079–1082.
(120) Sivula, K.; Ball, Z. T.; Watanabe, N.; Frechet, J. M. J. *Adv. Mater.* **2006**, *18* (2), 206–210.
(121) Patel, N. K.; Cina, S.; Burroughes, J. H. *IEEE J. Sel. Top. Quantum Electron.* **2002**, *8* (2), 346–361.
(122) Tang, C. W.; Vanslyke, S. A. *Appl. Phys. Lett.* **1987**, *51* (12), 913–915.
(123) Baldo, M. A.; O'Brien, D. F.; You, Y.; Shoustikov, A.; Sibley, S.; Thompson, M. E.; Forrest, S. R. *Nature* **1998**, *395* (6698), 151–154.
(124) Adachi, C.; Baldo, M. A.; Forrest, S. R.; Thompson, M. E. *Appl. Phys. Lett.* **2000**, *77* (6), 904–906.
(125) Duggal, A. R.; Foust, D. F.; Nealon, W. F.; Heller, C. M. *Appl. Phys. Lett.* **2003**, *82* (16), 2580–2582.
(126) Shtein, M.; Mahon, J. K.; Zhou, T.; Forrest, S. R.; Schwambera, M.; Meyer, N. *Solid State Technol.* **2002**, *45* (10), 18–18.
(127) Sun, Y. R.; Shtein, M.; Forrest, S. R. *Appl. Phys. Lett.* **2005**, *86* (11), 113504.
(128) Liu, J. S.; Kadnikova, E. N.; Liu, Y. X.; McGehee, M. D.; Frechet, J. M. J. *J. Am. Chem. Soc.* **2004**, *126* (31), 9486–9487.
(129) Uckert, F.; Tak, Y. H.; Müllen, K.; Bässler, H. *Adv. Mater.* **2000**, *12* (12), 905–908.
(130) Yan, H.; Scott, B. J.; Huang, Q.; Marks, T. J. *Adv. Mater.* **2004**, *16* (21), 1948–1953.
(131) Gong, X.; Wang, S.; Moses, D.; Bazan, G. C.; Heeger, A. J. *Adv. Mater.* **2005**, *17* (17), 2053–2058.
(132) Ma, W. L.; Iyer, P. K.; Gong, X.; Liu, B.; Moses, D.; Bazan, G. C.; Heeger, A. J. *Adv. Mater.* **2005**, *17* (3), 274–277.
(133) Lu, J.; Jin, Y.; Ding, J.; Tao, Y.; Day, M. *J. Mater. Chem.* **2006**, *16* (6), 593–601.
(134) Ma, B.; Lauterwasser, F.; Deng, L.; Zonte, C. S.; Kim, B. J.; Frechet, J. M. J. *Chem. Mater.* **2007**, *19* (19), 4827–4832.

(135) Tang, D.-F.; Wen, G.-A.; Qi, X.-Y.; Wang, H.-Y.; Peng, B.; Wei, W.; Huang, W. *Polymer* **2007**, *48* (15), 4412–4418.
(136) Liu, M. S.; Niu, Y. H.; Ka, J. W.; Yip, H. L.; Huang, F.; Luo, J. D.; Kim, T. D.; Jen, A. K. Y. *Macromolecules* **2008**, *41* (24), 9570–9580.
(137) Cheng, Y. J.; Liu, M. S.; Zhang, Y.; Niu, Y. H.; Huang, F.; Ka, J. W.; Yip, H. L.; Tian, Y. Q.; Jen, A. K. Y. *Chem. Mater.* **2008**, *20* (2), 413–422.
(138) Yang, R.; Xu, Y.; Dang, X.-D.; Nguyen, T.-Q.; Cao, Y.; Bazan, G. C. *J. Am. Chem. Soc.* **2008**, *130* (11), 3282–3283.
(139) Huang, F.; Cheng, Y.-J.; Zhang, Y.; Liu, M. S.; Jen, A. K. Y. *J. Mater. Chem.* **2008**, *18* (38), 4495–4509.
(140) Marc, B.; Rudolf, Z. *Macromol. Chem. Phys.* **2004**, *205* (12), 1633–1643.
(141) Yaqin, F.; Minghao, S.; Yonggang, W.; Zhishan, B.; Dongge, M. *J. Polym. Sci., Part A: Polym. Chem.* **2008**, *46* (4), 1349–1356.
(142) Ma, B.; Kim, B. J.; Deng, L.; Poulsen, D. A.; Thompson, M. E.; Frechet, J. M. J. *Macromolecules* **2007**, *40* (23), 8156–8161.
(143) Chen, J. P.; Markiewicz, D.; Lee, V. Y.; Klaerner, G.; Miller, R. D.; Scott, J. C. *Synth. Met.* **1999**, *107* (3), 203–207.
(144) Ping, W.; Chunpeng, C.; Qian, Y.; Fuzhi, W.; Zhihao, S.; Haiqing, G.; Xiaofang, C.; Xinghe, F.; Dechun, Z.; Qifeng, Z. *J. Polym. Sci., Part A: Polym. Chem.* **2008**, *46* (16), 5452–5460.
(145) Tao, Y.; Ma, B.; Segalman, R. A. *Macromolecules* **2008**, *41* (19), 7152–7159.
(146) Kim, K. D.; Park, J. S.; Kim, H. K.; Lee, T. B.; No, K. T. *Macromolecules* **1998**, *31* (21), 7267–7272.
(147) Lee, Y. Z.; Chen, X. W.; Chen, S. A.; Wei, P. K.; Fann, W. S. *J. Am. Chem. Soc.* **2001**, *123* (10), 2296–2307.
(148) Jin, S. H.; Kim, M. Y.; Kim, J. Y.; Lee, K.; Gal, Y. S. *J. Am. Chem. Soc.* **2004**, *126* (8), 2474–2480.
(149) Lu, S.; Liu, T. X.; Ke, L.; Ma, D. G.; Chua, S. J.; Huang, W. *Macromolecules* **2005**, *38* (20), 8494–8502.
(150) Xiao, X.; Fu, Y. Q.; Sun, M. H.; Li, L.; Bo, Z. S. *J. Polym. Sci., Polym. Chem.* **2007**, *45* (12), 2410–2424.
(151) Baldo, M. A.; O'Brien, D. F.; Thompson, M. E.; Forrest, S. R. *Phys. Rev. B* **1999**, *60* (20), 14422–14428.
(152) Furuta, P. T.; Deng, L.; Garon, S.; Thompson, M. E.; Frechet, J. M. J. *J. Am. Chem. Soc.* **2004**, *126* (47), 15388–15389.
(153) Deng, L.; Furuta, P. T.; Garon, S.; Li, J.; Kavulak, D.; Thompson, M. E.; Frechet, J. M. J. *Chem. Mater.* **2006**, *18* (2), 386–395.
(154) Tao, Y.; Ma, B.; Segalman, R. A. *Macromolecules* **2008**, *41* (19), 7152–7159.
(155) Kretzschmann, H.; Meier, H. *Tetrahedron Lett.* **1991**, *32* (38), 5059–5062.
(156) Yokoyama, A.; Yokozawa, T. *Macromolecules* **2007**, *40* (12), 4093–4101.
(157) Jeffries-El, M.; Sauve, G.; McCullough, R. D. *Macromolecules* **2005**, *38* (25), 10346–10352.
(158) Neef, C. J.; Ferraris, J. P. *Macromolecules* **2000**, *33* (7), 2311–2314.
(159) Iovu, M. C.; Jeffries-El, M.; Zhang, R.; Kowalewski, T.; Mccullough, R. D. *J. Macromol. Sci., Part A: Pure Appl. Chem.* **2006**, *43* (12), 1991–2000.
(160) Iovu, M. C.; Zhang, R.; Cooper, J. R.; Smilgies, D. M.; Javier, A. E.; Sheina, E. E.; Kowalewski, T.; McCullough, R. D. *Macromol. Rapid Commun.* **2007**, *28* (17), 1816–1824.
(161) Dittmer, J. J.; Marseglia, E. A.; Friend, R. H. *Adv. Mater.* **2000**, *12* (17), 1270–1274.
(162) Kline, R. J.; Mcgehee, M. D.; Toney, M. F. *Nat. Mater.* **2006**, *5* (3), 222–228.